Funded by the European Union

Project Title:

# Eco-operated, Modular, highly efficient, and flexible multi-POWERtrain for long-haul heavy-duty vehicles

Acronym: **EMPOWER**

Grant Agreement No.: **101096028**

| | |
|---|---|
| Topic: | **Modular multi-powertrain zero-emission systems for HDV (BEV and FCEV) for efficient and economic operation (2ZERO)** |
| Topic identifier: | **HORIZON-CL5-2022-D5-01-08** |
| Type of action: | **Innovation Action (IA)** |


| **Deliverable No.** | D3.2 | |
|---|---|---|
| **Deliverable Title** | Hydrogen storage | |
| **Deliverable Date** | 2024-10 → postponed to 2024-12 | |
| **Deliverable Type** | Report | |
| **Dissemination level** | Public | |
| **Written by** | Claudio MEZZA (IVECO)<br>Tobias LEINHOS (IVECO)<br>Paula LASTRA-DAME (ALSA)<br>Remi GONIN (ALSA)<br>Fouad AMMOURI (ALSA) | 2024-10-08<br>to<br>2024-12-10 |
| **Checked by** | Thomas BÄUML (AIT)<br>Dragan SIMIC (AIT) | 2024-12-11 |
| **Approved by** | Markus VILLINGER (VIL) | 2024-12-18 |
| **Status** | Version 0.1<br>Version 0.2<br>Version 1.0 | 2024-10-08<br>2024-12-11<br>2024-12-18 |

This project has received funding from the European Union's HORIZON EUROPE research and innovation programme under grant agreement No. 101096028. The content of this publication is the sole responsibility of the Consortium partners listed herein and does not necessarily represent the view of the European Commission or its services.

**Publishable Executive Summary**

As part of the EMPOWER project, the focus of this deliverable, D3.2, is the hydrogen storage system (HSS) of a fuel cell electric vehicle (FCEV). Considering the range requirement of 750 km and the other challenging constraints of the project (from the payload to the safety requirements), the selection of the system has been based on market readiness, customer needs, and actual regulations on hydrogen applications.
Various hydrogen storage methods are discussed, highlighting advantages and disadvantages, with compressed hydrogen being the preferred short-term solution for the EMPOWER project.
Moreover, a detailed description of main auxiliary components will be depicted (such as tanks, valves, sensors etc.), that are necessary to manage the system in driving condition and to monitor and control the refuelling/defueling processes.
Performance simulations have been conducted and are ongoing at vehicle level to optimize the power strategy between fuel cell and battery, aiming to match the performance of a baseline diesel truck.
Furthermore, the study investigates refuelling operation with a comprehensive evaluation done in collaboration with ALSA. With a proper simulation tool, developed by Air Liquide R&D, parametric and sensitivity analyses have been conducted. In particular, the investigation shows a prediction on average-volume gas quantities, such as temperature and pressure, during the refuelling, stabilization, or defueling phases of gaseous tanks.

This project has received funding from the European Union's HORIZON EUROPE research and innovation programme under grant agreement No. 101096028. The content of this publication is the sole responsibility of the Consortium partners listed herein and does not necessarily represent the view of the European Commission or its services.

This project has received funding from the European Union's HORIZON EUROPE research and innovation programme under grant agreement No. 101096028. The content of this publication is the sole responsibility of the Consortium partners listed herein and does not necessarily represent the view of the European Commission or its services.

**List of Figures**



**List of Tables**



This project has received funding from the European Union's HORIZON EUROPE research and innovation programme under grant agreement No. 101096028. The content of this publication is the sole responsibility of the Consortium partners listed herein and does not necessarily represent the view of the European Commission or its services.

**Abbreviations and Nomenclature**

Table 1: List of Abbreviations and Nomenclature

| Symbol or Shortname | Description |
|---|---|
| **0D** | Zero dimension |
| **1D** | One dimension |
| **APRR** | Average pressure ramp rate |
| **CHSS** | Compressed hydrogen storage system |
| **FCEV** | Fuel-cell electric vehicle |
| **H35HF** | 35 MPa high-flow |
| **SW** | Software |
| **H70** | 70 MPa |
| **HD** | Heavy-duty |
| **HMU** | Hydrogen management unit |
| **HRS** | Hydrogen refuelling station |
| **HSCU** | Hydrogen storage control unit |
| **HSS** | Hydrogen storage system |
| **LCA** | Life Cycle Assessment |
| **NWP** | Nominal working pressure |
| **P&ID** | Piping & Instrumentation diagram |
| **PRV** | Pressure relief valve |
| **RDI** | Refuelling data interface |
| **SAE** | Society of automotive engineers |
| **SOC** | State-of-charge |
| **TCO** | Total Cost of Operation |
| **TPC** | Thermal protective coating |
| **TPRD** | Thermally activated pressure relief device |
| **TVL** | Tank volume large |
| **ZE-HDV** | Zero-Emission Heavy-Duty Vehicles |

This project has received funding from the European Union's HORIZON EUROPE research and innovation programme under grant agreement No. 101096028. The content of this publication is the sole responsibility of the Consortium partners listed herein and does not necessarily represent the view of the European Commission or its services.

# 1 Introduction

The goal of Task 3.3 is to determine the most suitable hydrogen storage system (HSS) for the FCEV demonstrator to achieve a 750 km range while minimizing the impact on the vehicle's weight.
The activities of this task are going to be reported in this deliverable (D3.2). In order to deep dive into the behaviour of the system during refuelling/defueling, those operations have been simulated with a dedicated tool (see third chapter) and the results reported as a basis for the feature hardware data gathering.

Table 2: Timing of WP3.

| EMPOWER gantt chart | Year: | 2024 | | | | | | | | | | | | | | | |
|---|---|---|---|---|---|---|---|---|---|---|---|---|---|---|---|---|---|
| | Project quarter: | Q5 | | | Q6 | | | Q7 | | | Q8 | | | Q9 | | | |
| | Project month: | 13 | 14 | 15 | 16 | 17 | 18 | 19 | 20 | 21 | 22 | 23 | 24 | 25 | 26 | 27 | 28 |
| **WP3** | **Modular energy storages (battery and hydrogen tank)** | | | | | | | | | | | | | | | | |
| Task 3.1 | Hydrogen and battery topologies for FCEV and BEV demonstrators | | | | | | | | | | | | | | | | |
| Task 3.2 | Battery management systems for FCEV and BEV demonstrators | | | | | | | | | | | | | **D3.1** | | | |
| Task 3.3 | Hydrogen storage for FCEV | | | | | | | | | | **D3.2** | | | | | | |
| Task 3.4 | First level testing and validation of battery and battery management systems | | | | | | | | | | | | | | | | **D3.3** |

All these considerations are crucial for defining the HSS, ensuring a safe system that guarantees the needed range with an optimal weight distribution and payload capacity (comparable to a diesel truck).

The main key factors in defining the storage solution are:

- Vehicle architecture and packaging;
- Maximum range and performance;
- Respect of minimum clearances, particularly ground clearance;
- Safety requirements.

The suggested storage solution considers market readiness, actual customer needs, and the mitigation of the risks associated with a rapidly evolving technology. As it will be explained in the following chapters, the choice has been oriented on a compressed hydrogen storage system (CHSS) made of 5 tanks operating at 700 bar [1]. The hydrogen, due to the low enthalpy, independently if high pressure or liquid, needs stronger and more expensive tanks with respect to conventional fuels. Moreover, the flammability of the product and the severe conditions of use require particular attention to the aspects of safety. Table 3 [2] gives a high-level idea of the difference between hydrogen and other relevant fuels in trucks application.

This project has received funding from the European Union's HORIZON EUROPE research and innovation programme under grant agreement No. 101096028. The content of this publication is the sole responsibility of the Consortium partners listed herein and does not necessarily represent the view of the European Commission or its services.

Table 3: Fuel comparison for propulsion of trucks

| Fuel | Enthalpy content PCI MJ/m3 | Gaseous state | Physical state at 25 °C and 1 atm |
|---|---|---|---|
| **Hydrogen** | | | |
| Gas ambient conditions | 10,7 | 15 °C \| 1,013 bar | Gas |
| Gas at 200 bar | 1.853 | 15 °C \| 200 bar | Gas |
| Gas at 700 bar | 4.500 | 15 °C \| 700 bar | Gas |
| Liquid at -253 °C | 8.491 | - | Liquid |
| **Methane** | | | |
| Gas ambient conditions | 32,56 | 15 °C \| 1,013 bar | Gas |
| Gas at 200 bar | 6.860 | 15 °C \| 200 bar | Gas |
| Liquid at -160 °C | 20.920 | - | Liquid |
| **Gasoline** | 31.150 | - | Liquid |

The main options for storing $H_2$ are compressed (350 or 700 bar), liquid, sub-cooled liquid and cryo-compressed [3]. To highlight the main advantages and disadvantages of each solution, a short description of the main traits is given below:

- **Compressed Hydrogen (CgH2)**:
  - **350 bar**: This technology is already available and it is used in applications like buses and heavy-duty vehicles. It offers lower storage costs but has a lower density, resulting in a shorter range.
  - **700 bar**: This is expected to be the mainstream for passenger cars and light-duty vehicles. It provides a higher storage density and longer range but comes with higher storage costs and energy requirements for compression.
- **Liquid Hydrogen (LH2)**:
  - It has a higher energy density than compressed hydrogen, making it suitable for applications requiring longer ranges. However, it requires advanced insulation and management of boil-off losses during storage. The technology is still not mature to be applied in field tests.

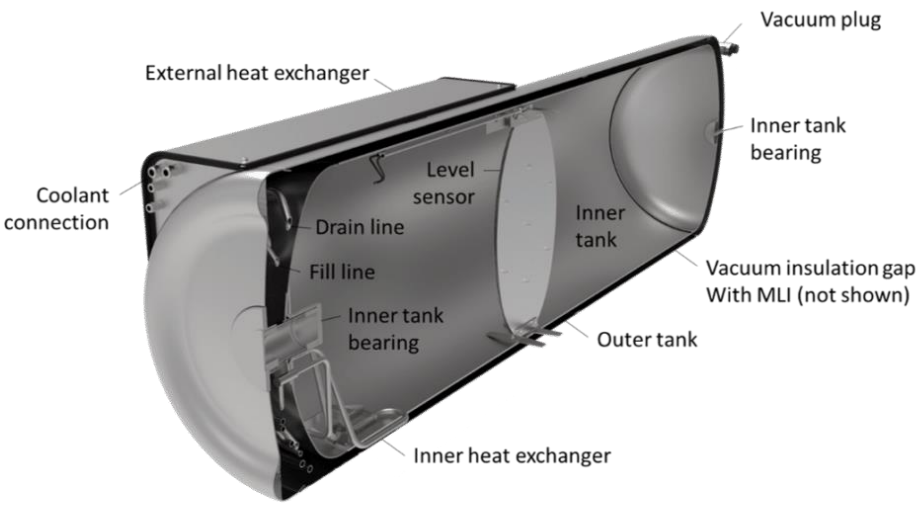


Figure 1: Liquid tank from SAG [4].

This project has received funding from the European Union's HORIZON EUROPE research and innovation programme under grant agreement No. 101096028. The content of this publication is the sole responsibility of the Consortium partners listed herein and does not necessarily represent the view of the European Commission or its services.

The main features of liquid storage technology are [4]:

- Thermo flask principle – inner and outer tank
- High Vacuum and multi layer insulation
- Hydrogen storage at -250 °C and low pressure < 10 bar
- Density increase gas-liquid at 273 K and 1 bar factor 700
- 30 % higher volumetric energy density than 700 bar
- Hold time 9 days until boil off pressure 5 bar

- **Sub-cooled Liquid Hydrogen (sLH2)** [5]:
  It offers approximately 50 % higher density compared to compressed hydrogen at 700 bar. It uses insulated stainless steel low-pressure tanks, which are lighter and cheaper. The technology is being developed by some OEMs and Engineering companies.
- **Cryo-compressed Hydrogen (CcH2)**:
  It combines the principles of compressed and liquid hydrogen storage, allowing hydrogen to be stored at elevated pressures and low temperatures. This method results in higher storage efficiency and density but requires advanced insulation and management of boil-off losses.

For an application like EMPOWER, in which the aim of the project is a field demonstration, and the HD truck will be handed-over to a customer, the compressed solution is the best short-term and safe technology. On one hand, the refuelling technology already exists, and the refuelling protocols are already available. On the other hand, this solution needs a large storage on board because, compared to liquid $H_2$, it offers a lower energy density.
It is well known that one of the limits of the hydrogen is the low density in normal temperature and pressure, so, for an efficient storage, hydrogen density needs to be increased by reducing the volume under normal temperature and pressure conditions.
As previously described, hydrogen tanks in vehicles typically store compressed hydrogen at either 350 bar (5,000 psi) or 700 bar (10,000 psi). The main parameters related to this kind of hydrogen tank are [6]:

1. Tank inner volume in litres
2. Operating storage pressure in bar or pascal
3. Mass of hydrogen stored at the operating storage pressure in kg
4. Operating temperature range in °C
5. Maximum allowable pressure in bar or pascal
6. Mass of the tank in kg
7. External dimensions
8. Number of cycles allowed before overhaul
9. Certifications obtained for the vessel
10. Tank type

Regarding the last point, there are currently four commercially available types of hydrogen tanks (see also Figure 2), each differing in materials and pressure resistance [6] [3]:

- **Type I:** Tanks are made of metal (usually aluminium) and the main driver is the cost since they do not have any additional wrap, maintaining the construction very simple.
- **Type II:** Tanks have composite material reinforcement that allows higher pressure without significantly increasing the thickness of the material. This brings an advantage in terms of weight.
- **Type III:** Tanks are fully wrapped with composite materials and have a metal liner usually quite thin, in fact the bearing of the pressure is mainly in charge of the synthetical wrapping.

This project has received funding from the European Union's HORIZON EUROPE research and innovation programme under grant agreement No. 101096028. The content of this publication is the sole responsibility of the Consortium partners listed herein and does not necessarily represent the view of the European Commission or its services.

- **Type IV:** Tanks feature a polymer liner, and they can bear high pressure without a big increase of weight. This feature makes Type IV tanks the best ones if a high quantity of hydrogen needs to be stored at high pressure without dramatically increasing weight.

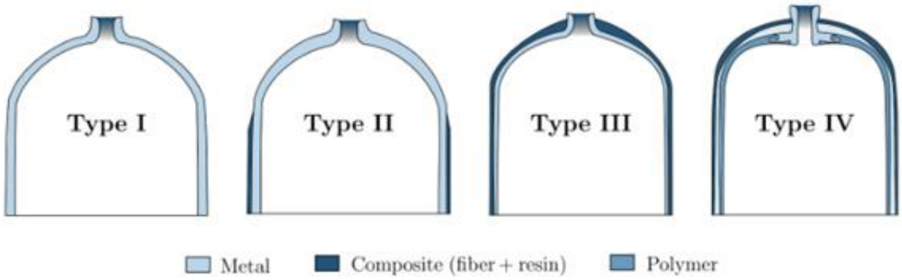


Figure 2: Comparison between different compressed hydrogen tanks [7].

The tanks selected for the EMPOWER application are five Type IV, which are the best in terms of performances.

The refuelling process at hydrogen filling stations is monitored and controlled by a Hydrogen Storage Control Unit (HSCU) [8], that takes care of the

- tank pressure regulation;
- hydrogen gas concentration monitoring/warning;
- monitoring of the refuelling process and communication with the filling station;
- monitoring of critical tank parameters and reaction to limit values;
- communication with the fuel cell control system;
- information of the driver about the system status and range.

Figure 3: Example of HSCU from Bosch [9].

As far as it concerns the supply chain of the hydrogen, this is one of the main challenges in the adoption of zero emission heavy duty vehicles (ZE-HDVs). Vehicles lack a sufficient refuelling infrastructure, which limits their usability to a small area unless an expensive hydrogen generator is purchased.
Even the cost of transporting hydrogen from the exporting to the importing region can be substantial, and so assessing the total cost of supply – for production and transport – is essential. Depending on the carrier and the transport distance, transport costs can shift the competitiveness in favour of domestic production.
The cheapest solution seems to be represented by compressed hydrogen via pipeline which could be the most competitive option in terms of costs.

This project has received funding from the European Union's HORIZON EUROPE research and innovation programme under grant agreement No. 101096028. The content of this publication is the sole responsibility of the Consortium partners listed herein and does not necessarily represent the view of the European Commission or its services.

## 2 Hydrogen Storage System in EMPOWER

The compressed gaseous hydrogen storage system selected in EMPOWER consists of five Type IV composite cylindrical pressure vessels (containers) with a nominal working pressure (NWP) of 700 bar. The maximum range to define the number and dimension of the tanks has been assessed based on the estimated hydrogen consumption for long-haul use. As the project aims to cover the corridor between Italy and Germany via the Brenner Pass, specific simulations are being conducted to determine the optimal power strategy between fuel cell and battery to achieve performance comparable to a baseline diesel truck. Figure 4 illustrates one of the simulation results, where the orange curve represents the target speed of a diesel truck, the blue curve shows the speed of the simulated FCEV, and the yellow curve indicates the battery's state of charge. The yellow curve is important for assessing the number of batteries, in fact using two batteries would be ideal for energy storage, providing over 100 kWh of available energy. However, using a single battery could significantly reduce the vehicle's total weight, leading to better consumption and increased payload capacity for the customer. This option is currently being evaluated. The results suggest anyway that the solution can match diesel performance with minor optimizations in SW energy management.

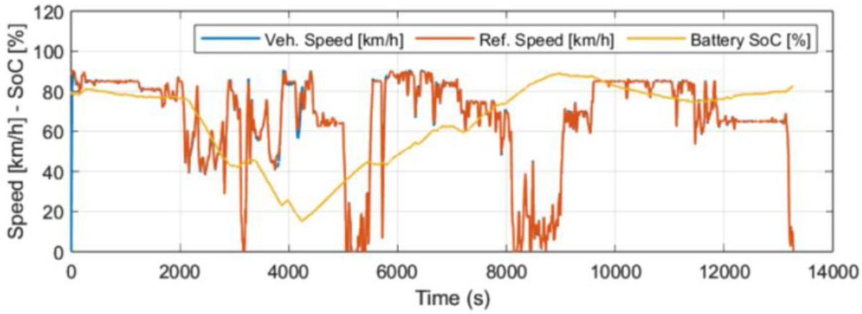


Figure 4: Example of simulation Verona-Ulm over the Brenner Pass.

All five containers are dimensionally identical (D = ~600 mm x L = 2050 mm) and store a total hydrogen gas capacity of 73 kg at 700 bar at 15°C on the vehicle. Each container contains an electrically actuated normally closed solenoid valve, check valve, filters, excess flow valve, two thermally activated pressure relief devices (TPRDs) at the tank end bosses, two internal gas temperature sensors, and a pressure sensor. Each container includes a thermal protective coating (TPC) applied to the cylindrical portion of the vessel (dome protection) that enhances and extends the thermal resistance of the container in a vehicle fire. The TPRD venting ports are individually routed with dedicated stainless steel hard lines to outer points on the vehicle in compliance with regulation and include vent caps that prevent environmental elements to penetrate during normal vehicle use.

This project has received funding from the European Union's HORIZON EUROPE research and innovation programme under grant agreement No. 101096028. The content of this publication is the sole responsibility of the Consortium partners listed herein and does not necessarily represent the view of the European Commission or its services.

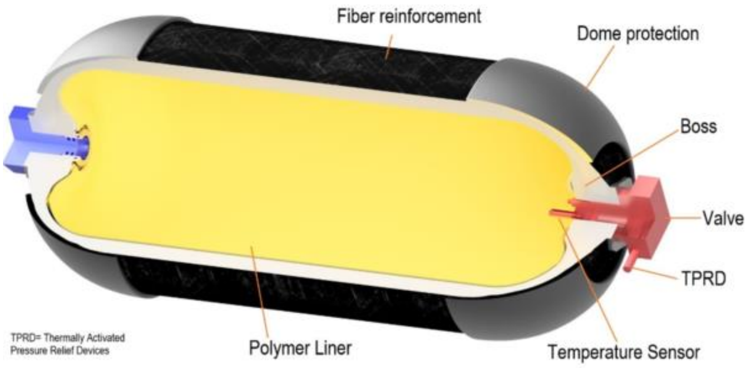


Figure 5: Schematic of compressed tank from ECS [10].

The five tanks are fluidly connected via a central manifold that receives hydrogen from one of the two tank fuelling receptacles. They have connection geometries H70 and H35HF according to ISO 17268 and distribute hydrogen to all five tanks. During vehicle operation, when the solenoid valves are activated and open, they receive hydrogen from the five tanks and distribute it to a pressure control unit. This unit consists of a multi-stage pressure reduction to the fuel cell system, a manifold pressure measurement, a pressure measurement for the fuel cell system supply and a pressure relief valve for the fuel cell supply. This is activated in the event of a pressure reduction failure and has a vent connection that is led to an external point on the vehicle with a special stainless-steel liner in accordance with regulations. A vent cap prevents the ingress of environmental elements during normal vehicle use.

The vehicle sensor system detects a hydrogen concentration in air using four hydrogen concentration detectors mounted as follows:

1. in-cab, cab interior roof;
2. below cab, above fuel cell system;
3. above hydrogen storage on driver side in back-of-cab assembly and
4. above hydrogen storage on passenger side in back-of-cab assembly.

The hydrogen detectors are electrically connected to the hydrogen management unit (HMU) and relays the required warnings and alarms to the driver interface instrument cluster as defined by regulation (UN ECE R134). In addition, the hydrogen storage system includes a service defueling function which includes tool operated manual valves on each container as well as a manually operated service defueling valve fluidly connected to the manifold and normally capped with a blind plug-in normal vehicle usage.

### 2.1 Tanks and auxiliary components

Table 4: List and specifications of HSS main components

| Component | Quantity in System: | Picture | Homologation / Certificates |
|---|---|---|---|
| Hydrogen Tank | 5 | 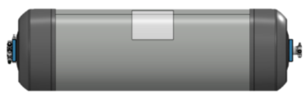 | UN ECE R134<br>EU 2021/535 Annex XIV |
| On-Tank Valve | 5 |  | UN ECE R134<br>EU 2021/535 Annex XIV<br>HGV3.1<br>HPRD1 |

| | | | |
|---|---|---|---|
| End Plug | 5 |  | UN ECE R134<br>EU 2021/535 Annex XIV |
| H70 Receptacle | 1 |  | EC79<br>ISO 17268-1 |
| H35HF Receptacle | 1 | | EC79<br>ISO 17268-1 |
| Fuel Manifold | 1 |  | - |
| Pressure Regulator | 1 |  | EC79<br>EU 2021/535 Annex XIV<br>HGV3.1 |
| Fuel Lines and Fittings | Multiple |  | EC79 |
| H2 Detectors | 4 |  | - |

## 2.2 Layout

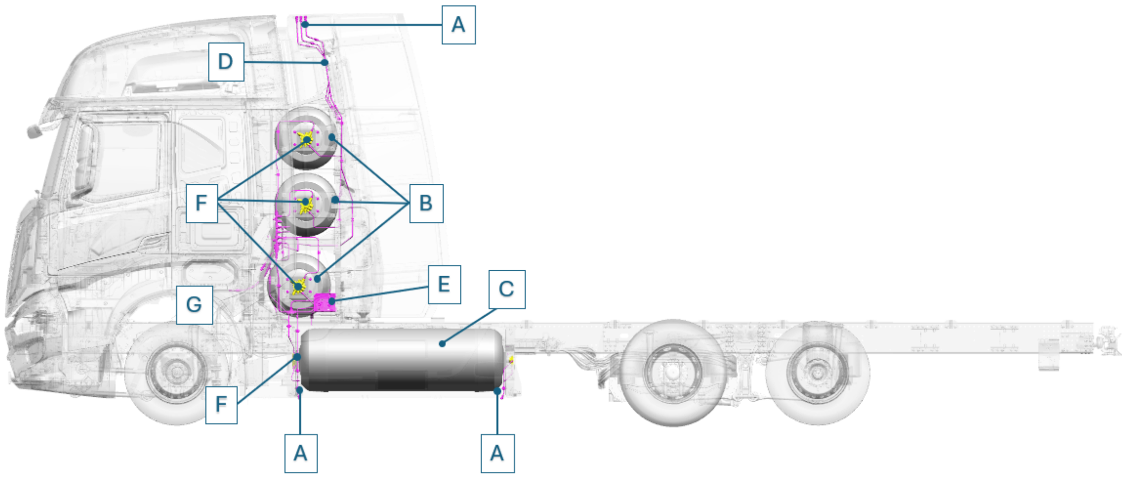


This project has received funding from the European Union's HORIZON EUROPE research and innovation programme under grant agreement No. 101096028. The content of this publication is the sole responsibility of the Consortium partners listed herein and does not necessarily represent the view of the European Commission or its services.

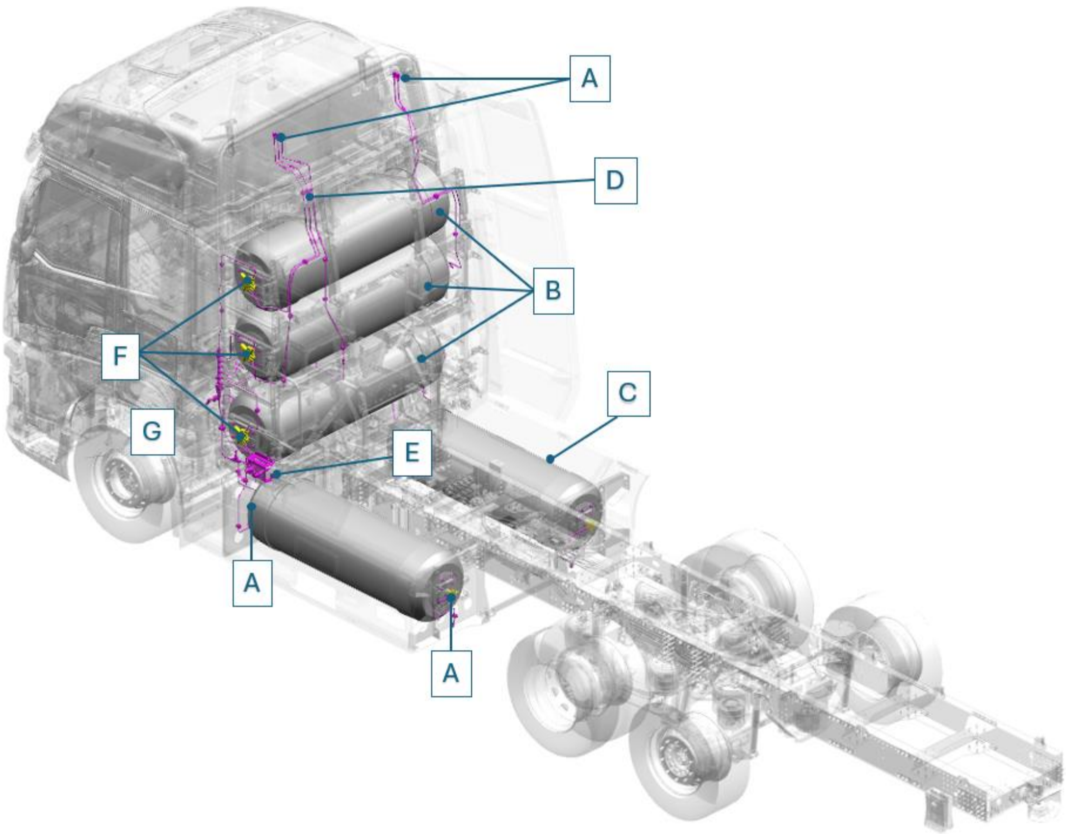


Figure 6: Vehicle Hydrogen Storage System Integration onto the IVECO S-eWay H2 HD truck.

A. TPRD Vent Outlets (upper & lower)
B. CHSS Containers (back of cab) (x 3)
C. CHSS Containers (side saddle positions) (x 2)
D. Hydrogen Vent Lines, TPRDs and PRV
E. Hydrogen Refuelling Receptacles, Driver Side (H70 and H35HF)
F. On-Tank Valves with integrated thermally-activated pressure relief devices
G. Service Defueling Valve

This project has received funding from the European Union's HORIZON EUROPE research and innovation programme under grant agreement No. 101096028. The content of this publication is the sole responsibility of the Consortium partners listed herein and does not necessarily represent the view of the European Commission or its services.

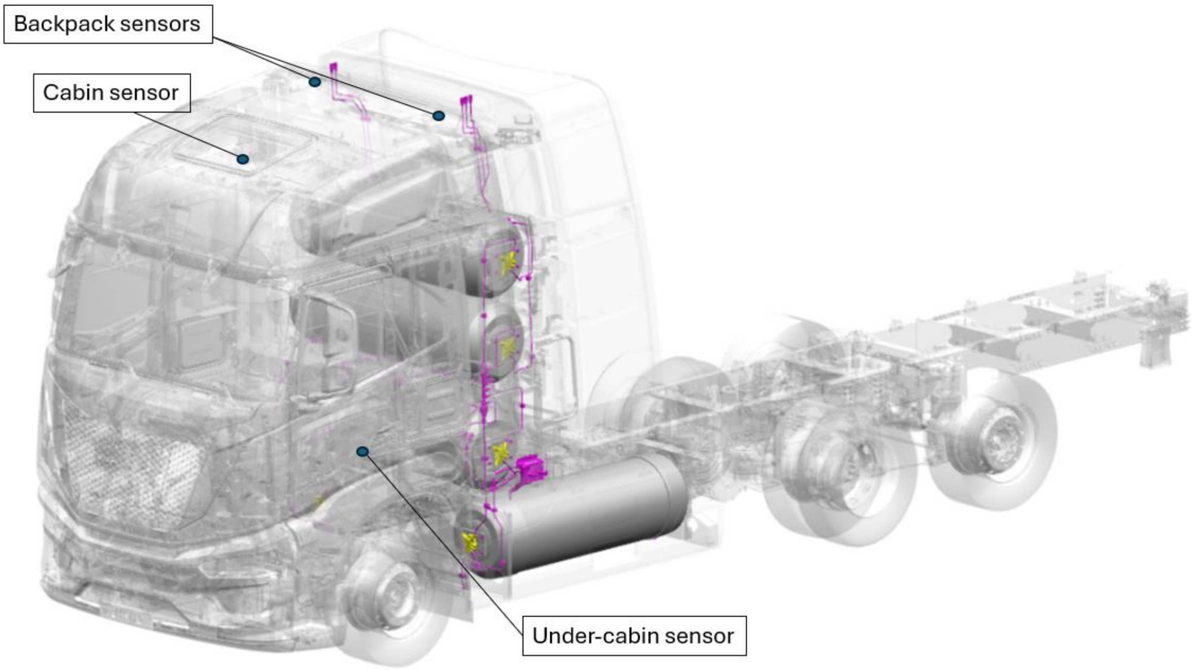


Figure 7: Sensors for hydrogen concentration detection.

The refuelling door assembly contains two hydrogen receptacles, H70 and H35HF with refuelling data interface (RDI) transmitters and are mounted on the driver's side of the vehicle. The fuelling door includes a locking latch as well as position sensor which is used by the HSCU to allow the vehicle to go into and out of fuelling mode. While in fuelling mode, the vehicle will communicate storage system parameters such as the refuelling interface (H70, H35), the storage system hydrogen pressure and temperature, and the system capacity to the hydrogen station which in turn will select the appropriate fuelling protocol to target a maximum (100 %) fuelling.


Figure 8: View of the fuelling door assembly open with the H70 (left) and H35HF (right) receptacles with RDI transmitters.

### 2.3 Back-pack and chassis brackets

The $H_2$ tank chassis integration is realised by two lateral side saddle $H_2$ tanks and three vertically staggered $H_2$ tanks in a backpack structure behind the cabin.

This project has received funding from the European Union's HORIZON EUROPE research and innovation programme under grant agreement No. 101096028. The content of this publication is the sole responsibility of the Consortium partners listed herein and does not necessarily represent the view of the European Commission or its services.

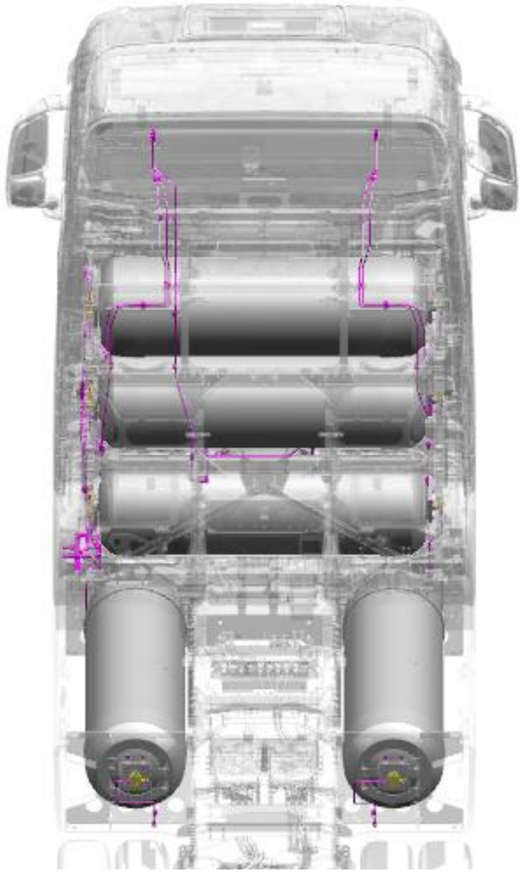

Figure 9: Rear view backpack and lateral frames to fix $H_2$ tanks.

The side saddle tanks are neck mounted, in between a front and a rear frame bracket. To reduce the shear force in a possible side crash event a deformable crash element is implemented to the mounting structure.
The side tank fixation brackets as well as the overall installation have been virtually validated according to the endurance run mission profiles and durability loads to cover accelerations in X, Y and Z as well as chassis torsion scenarios. Side crash simulations according to ECE R134 have been accomplished.

While the side saddle tanks only have the function to provide a $H_2$ storage compartment, the backpack structure provides additional functionalities. Main function is to provide $H_2$ storage. The backpack structure is split into three modules, allowing the accessibility to each single tank for service activities. In addition, the structure provides the interface to the thermal cooling unit located on top of the backpack. Furthermore, the backpack includes the fuelling interface, providing the possibility to fuel the tanks via a 350 bar and a 700 bar filling receptacle. Most of the $H_2$ fuel line system is packaged in the backpack leaving only the $H_2$ fuel line to the side saddle tanks chassis mounted. The same applies to the $H_2$ tank vent line system, which is routed from each $H_2$ fuel tank up to the very top of the backpack to vent the tanks in case of a crash event or fire.
Finally, the backpack provides the interfaces to the aerodynamic covers as well as the access system and trailer connection auxiliaries in case of an articulated truck application.
Target weight of the backpack structure is approximately 400 kg, ending up at an estimated overall weight of 1.2 - 1.3 t for the complete backpack unit, including the $H_2$ storage system, cooling unit and aerodynamic cover.

The structure will be virtually validated considering the endurance run mission profiles and durability loads to cover accelerations in X, Y and Z as well as chassis torsion scenarios. Crash simulation will be carried out according to ECER29.03.

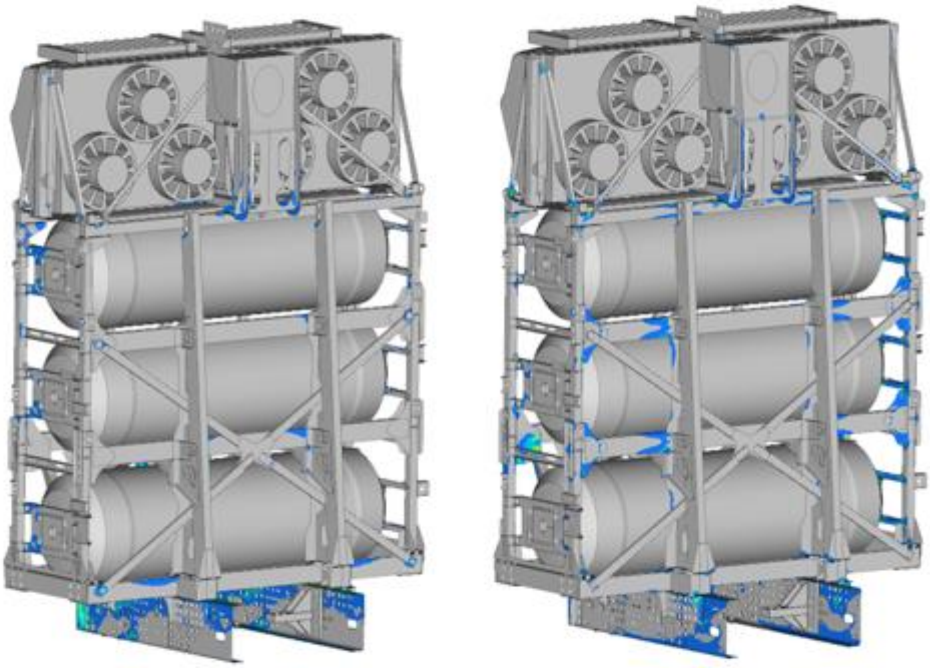

Figure 10: Examples of stress distribution outputs - durability simulation according to mission profiles.

This project has received funding from the European Union's HORIZON EUROPE research and innovation programme under grant agreement No. 101096028. The content of this publication is the sole responsibility of the Consortium partners listed herein and does not necessarily represent the view of the European Commission or its services.

# 3 Case study

## 3.1 Motivation

As previously mentioned, the five tanks of the FCEV demonstrator are located at the back of the driver's cabin. For each tank, the piping line connecting it to the dispenser will differ. This implies that the head or pressure loss of the different pipings will also differ. This can induce a difference of refuelling rates among the tanks during the refuelling of the FCEV. A discrepancy of refuelling rates leads to a discrepancy of temperatures inside the tanks. Also, depending on the HRS hose and nozzle, the refuelling rate will be affected.

To ensure safety during the refuelling, the standard SAE J2601 [11] recommends maintaining the inner gas temperature between -40 °C and 85 °C. Estimating the worst case in term of temperature elevation inside the tanks, i.e. the hot case, is beneficial to avoid overheating during the refuelling.

Accordingly, the objective of this study is to investigate the influence of the head loss on the temperature rise inside the tank. To perform this study:

- a standard refuelling will be defined;
- refuelling scenarios will be simulated with OneSOFIL, an Air Liquide tool, using different head loss coefficients extracted from HRS hose and nozzle;
- a hot case will be identified from the simulation results.

## 3.2 Simulation software

The software OneSOFIL [12] [13] (One SOftware for FILling) is a simulation tool developed by Air Liquide R&D. It is a 0D model in the gas and 1D model in the tank walls. This tool aims to quickly, in a few minutes, predict volume-average gas quantities, e.g. temperature, pressure and surface-average wall temperatures during the refuelling, stabilisation or defueling phases of gaseous tanks. It allows to perform parametric studies and sensitivity analyses studies.

The current version is compatible for pure gas. The modelling for the hydrogen refuelling case has been validated using experimental data from the European projects HyTransfer [14] and PrHyde [15].

### 3.2.1 Physical system

In OneSOFIL, the physical system considered is:

1. the dispenser;
2. the piping from the dispenser of the HRS to one tank;
3. a single tank.

Figure 11 gives an illustration of the physical system considered.

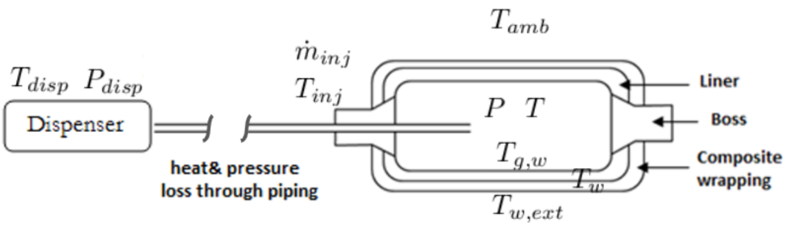


Figure 11: Physical system considered in OneSOFIL software.

Inputs to the software are the pressure $P_{disp}$ and temperature $T_{disp}$ measured at the dispenser. From the difference of pressures between the dispenser and the tank, the mass flow injected into the tank $\dot{m}_{inj}$ is

This project has received funding from the European Union's HORIZON EUROPE research and innovation programme under grant agreement No. 101096028. The content of this publication is the sole responsibility of the Consortium partners listed herein and does not necessarily represent the view of the European Commission or its services.

deduced. By considering the heat exchanged between the piping and the ambient environment, an injection temperature $T_{inj}$ is deduced from the dispenser temperature. From the mass flow and the injection temperature, a pressure P and temperature T of the gas inside the tank can be predicted, as well as temperatures in walls $T_w$ (e.g. at the interface between the gas and the inner walls $T_{g,w}$ and at the interface between the external walls and the ambient environment $T_{w,ext}$).

### 3.2.2 Physical modelling

#### 3.2.2.1 Piping pressure drop modelling

This section aims to detail the mathematical relations used to extract a mass flow from the difference of pressures between the dispenser and the tank.

In OneSOFIL, the pressure drop in the piping, i.e. the pressure drop through the different valves, piping elbows, restrictions, etc, is modelled with an equivalent valve. This valve is characterised by a head loss coefficient $k_v$ [$m^3/h$]. Then, depending on the difference of pressures between the dispenser and the tank, the mass flow is deduced, as follows:

for a subsonic flow in the valve, i.e. $2P_{tank} > P_{disp}$ , then,

$$\dot{m}_{inj} = 514\, k_v \sqrt{\frac{\rho_N (P_{disp} - P_{tank}) P_{tank}}{T_{disp}}} \quad , \tag{1}$$

and for a supersonic flow in the valve, i.e. $2P_{tank} < P_{disp}$ , then,

$$\dot{m}_{inj} = 257\, k_v\, P_{disp} \sqrt{\frac{\rho_N}{T_{disp}}} \quad , \tag{2}$$

with $\rho_N$ [$kg/m^3$] the density of hydrogen at normal condition, i.e. 1 atm and 0 °C.

#### 3.2.2.2 Tank modelling

In this section the focus is on modelling inside the tank. OneSOFIL modelling is based on thermodynamical considerations. The gas is assumed to be a uniform volume, i.e. a 0-dimension (0D) region and the walls are discretised in radial direction, i.e. 1-dimension (1D).

In the gas, the governing equations are the mass (3) and energy balance equations (4),

$$\frac{dm}{dt} = \dot{m}_{inj}, \tag{3}$$

$$mc_p \frac{dT}{dt} = VT\beta \frac{dP}{dt} + k_g S_{w,int}(T_{g,w} - T) + \dot{m}_{inj}\left(h(P, T_{inj}) + \frac{u_{inj}^2}{2} - h(P,T)\right), \tag{4}$$

where m [kg] is the internal gas $\dot{m}_{inj}$ [kg/s] is the injected mass flow, T [K] is the internal gas temperature, P [Pa] is the gas pressure, V [$m^3$] is the tank volume, $\beta$ [1/K] is the isochoric expansion coefficient, $c_p$ [J/kg/K] is the gas specific heat capacity, h [J/kg] is the gas specific enthalpy, $T_{inj}$ [K] is the injection temperature and $u_{inj}$ [m/s] is the injection velocity.

The term $k_g S_{w,int}(T_{g,w} - T)$ models the heat exchanged with the walls. $T_{g,w}$ [K] is the internal tank wall temperature, $S_{w,int}$ [$m^2$] is the internal tank wall surface in contact with the gas and $k_g$ [$W/m^2/K$] is the heat transfer coefficient between the gas and the wall.

A real gas equation of state completes this equation set,

This project has received funding from the European Union's HORIZON EUROPE research and innovation programme under grant agreement No. 101096028. The content of this publication is the sole responsibility of the Consortium partners listed herein and does not necessarily represent the view of the European Commission or its services.

$$PV = \frac{m}{M_{H_2}} Rz(P,T)T \tag{5}$$

where z [1] is the compressibility factor, $M_{H_2}$ [kg/mol] is the molar mass of hydrogen and R [1/mol/K] is the ideal gas law constant.

The tank walls are composed of two layers of constant thickness and different physical properties representing the liner layer and the carbon wrap liner around the gaseous volume. It is assumed that the wall is 1D, i.e. the thermal diffusion is only modelled in the tank radial direction.

The governing equation is the energy balance equation (6),

$$\rho_w c_{p,w} \frac{\partial T_w}{\partial t} = \frac{\lambda_w}{r} \frac{\partial}{\partial r}\left(r \frac{\partial T_w}{\partial r}\right), \tag{6}$$

where $\rho_w$ [kg/m$^3$] is the density, $c_{p,w}$ [J/kg/K] is the specific heat capacity, and $\lambda_w$ [W/m$^2$/K] is the heat conductivity of a wall layer. The variable r [m] is the radial direction.

The external wall layer in contact with the ambient environment exchanges (i) a radiative heat flux $\phi_{rad}$ [W],

$$\phi_{rad} = \varepsilon\sigma S_{w,ext}\left(T_{amb}^4 - T_{w,ext}^4\right), \tag{7}$$

where ε [1] is the emissivity coefficient, $\sigma$ [W/m$^2$/K$^2$] is the Stefan Boltzmann constant, and $S_{w,ext}$ [m$^2$] is the external tank wall surface in contact with the ambient environment, and (ii) a heat flux from natural convection $\phi_{conv}$ [W],

$$\phi_{conv} = k_a S_{w,ext}\left(T_{amb} - T_{w,ext}\right), \tag{8}$$

where $k_a$ [W/m$^2$/K] is the heat transfer coefficient between external wall and the ambient environment.

### 3.3 Tank geometrical and material properties for the simulation

The geometrical and material properties of the tank used for the simulation is reported in Table 5. For the composite (carbon wrap), data from the hot case tank of the SAE 2601 [11] are selected.

The geometrical and material properties of the piping used for the simulation is reported in Table 6.

Table 5: Geometrical and thermophysical tank parameters.

| | | |
|---|---|---|
| Water volume | 363 | L |
| Nominal working pressure | 700 | bar(g) |
| Inner tank diameter | CONFIDENTIAL | mm |
| Liner thickness | CONFIDENTIAL | mm |
| Composite thickness | CONFIDENTIAL | mm |
| Liner density* | 1130 | kg/ m3 |
| Liner specific heat capacity* | 1646 | J/kg/K |
| Liner thermal conductivity* | 0.2575 | W/K/m |
| Composite density** | 1494 | kg/ m3 |
| Composite specific heat capacity** | 1120 | J/kg/K |
| Composite thermal conductivity** | 0.5 | W/K/m |
| Emissivity for tank external surface | 0 | no unit |

*The liner material selected is Nylon PA6 [16].
**The composite material properties are issued from the hot case tank of the SAE J2601 [11].

This project has received funding from the European Union's HORIZON EUROPE research and innovation programme under grant agreement No. 101096028. The content of this publication is the sole responsibility of the Consortium partners listed herein and does not necessarily represent the view of the European Commission or its services.

Table 6: Geometrical and thermophysical piping parameters.

| | | |
|---|---|---|
| Piping inner diameter (injection diameter) | CONFIDENTIAL | mm |
| Average inner piping diameter* | 6 | mm |
| Length piping * | 11.4 | m |
| Mass * heat Capacity (m*cp) piping * | 8500 | J/K |

*Data issued from SAE J2601 [11].

### 3.4 Reference refuelling case

As previously mentioned, in this study, a standard refuelling case is needed. Due to its common use, the lookup-table protocol issued from the SAE J2601 [11] and J2601 TIR 5 [17] is selected. To use the lookup-table protocol some parameters must be defined in advance. A precooling capacity must be selected, e.g. T20, T30, or T40 (i.e. -20°C, -30°C and -40°C). The mean value is selected.

→ Pre-cooling category: **T30**

The FCEV volume category is D (total tank volume > 256 litres) and the unitary tank volume is superior to 250 litres (TVL > 250 litres). As there is a communication between the FCEV demonstrator and the HRS the corresponding SAE lookup-table is the following:

Table 7: Look-up table for tank category D, 250 litres < TVL < 800 litres, 700 bar refuelling and precooling capacity of -30°C. The table is issued from the standard SAE J2601-5 [17].

***Table G10 - H70-T30D: Capacity Category D communications, 250 < TVL ≤ 800 L***

| H70-T30D Capacity Category D comm 250 < TVL ≤ 800 L | APRR [MPa/min] | Target Pressure Ptarget [MPa] | Target Pressure Top-Off [MPa] | Top-Off-APRR [MPa/min] | Target Pressure, $P_{target}$ [MPa] | | | | | | | | | | | |
|---|---|---|---|---|---|---|---|---|---|---|---|---|---|---|---|---|
| | | Initial Tank Pressure, $P_0$ [MPa] | | | | | | | | | | | | | | |
| | | 0,5 - 5 (no interpolation) | | | 0,5 | 2 | 5 | 10 | 15 | 20 | 30 | 40 | 50 | 60 | 70 | > 70 |
| Ambient Temperature, $T_{amb}$ [°C] >50 | no fueling | no fueling | no fueling | no fueling | no fueling | no fueling | no fueling | no fueling | no fueling | no fueling | no fueling | no fueling | no fueling | no fueling | no fueling | no fueling |
| 50 | 1,8 | 53,3 | 87,5 | 1,0 | see Top-Off | see Top-Off | 80,8 | 87,1 | 86,9 | 86,5 | 85,7 | 84,8 | 83,7 | 82,5 | 81,0 | no fueling |
| 45 | 3,6 | 70,3 | 87,5 | 1,0 | see Top-Off | see Top-Off | 81,4 | 87,1 | 86,7 | 86,3 | 85,3 | 84,1 | 82,8 | 81,4 | 79,6 | no fueling |
| 40 | 5,6 | 70,8 | 87,5 | 1,3 | see Top-Off | see Top-Off | 81,3 | 87,0 | 86,5 | 86,0 | 84,7 | 83,4 | 81,8 | 80,2 | 78,1 | no fueling |
| 35 | 5,9 | 70,7 | 87,5 | 1,2 | see Top-Off | see Top-Off | 81,2 | 87,1 | 86,5 | 86,0 | 84,7 | 83,3 | 81,8 | 80,1 | 78,1 | no fueling |
| 30 | 7,5 | 69,1 | 87,5 | 1,6 | see Top-Off | see Top-Off | 81,3 | 87,0 | 86,4 | 85,7 | 84,3 | 82,7 | 81,1 | 79,2 | 77,1 | no fueling |
| 25 | 9,2 | 67,3 | 87,5 | 2,0 | see Top-Off | see Top-Off | 81,2 | 86,9 | 86,2 | 85,5 | 83,9 | 82,1 | 80,3 | 78,3 | 76,1 | no fueling |
| 20 | 10,9 | 65,3 | 87,5 | 2,5 | see Top-Off | see Top-Off | 81,3 | 86,8 | 86,0 | 85,2 | 83,4 | 81,5 | 79,5 | 77,4 | 75,0 | no fueling |
| 10 | 14,0 | 61,6 | 87,5 | 3,0 | see Top-Off | see Top-Off | 81,1 | 86,8 | 85,7 | 84,7 | 82,6 | 80,5 | 78,3 | 76,0 | 73,4 | no fueling |
| 0 | 22,0 | 55,0 | 87,5 | 6,3 | see Top-Off | see Top-Off | 87,3 | 86,0 | 84,7 | 83,5 | 80,9 | 78,3 | 75,7 | 73,1 | no fueling | no fueling |
| -10 | 22,2 | 58,0 | 87,5 | 6,4 | see Top-Off | see Top-Off | 87,0 | 85,8 | 84,5 | 83,2 | 80,7 | 78,1 | 75,5 | 72,9 | no fueling | no fueling |
| -20 | 22,2 | 62,0 | 87,5 | 6,2 | see Top-Off | see Top-Off | 86,8 | 85,6 | 84,3 | 83,0 | 80,4 | 77,9 | 75,3 | 72,7 | no fueling | no fueling |
| -30 | 22,2 | 66,0 | 87,5 | 5,9 | see Top-Off | see Top-Off | 86,6 | 85,3 | 84,1 | 82,8 | 80,2 | 77,7 | 75,1 | 72,6 | no fueling | no fueling |
| -40 | 22,2 | 70,0 | 87,5 | 5,3 | see Top-Off | see Top-Off | 86,4 | 85,2 | 83,9 | 82,6 | 80,0 | 77,5 | 75,0 | 72,5 | no fueling | no fueling |
| <-40 | no fueling | no fueling | no fueling | no fueling | no fueling | no fueling | no fueling | no fueling | no fueling | no fueling | no fueling | no fueling | no fueling | no fueling | no fueling | no fueling |

An ambient temperature must be selected from -40 °C to 50 °C. To avoid using interpolated values, 20°C is selected.

→ **Tamb = 20°C.**

Using values in Table 7, the corresponding average pressure ramp rate (APRR) is 10.9 MPa/min until $P_{disp} = 65.3\ MPa$ and then 2.5 MPa/min until $P_{disp} = 87.5\ MPa$.

This project has received funding from the European Union's HORIZON EUROPE research and innovation programme under grant agreement No. 101096028. The content of this publication is the sole responsibility of the Consortium partners listed herein and does not necessarily represent the view of the European Commission or its services.

→ **APRR = 10.9 MPa/min, Pdisp < 65.3 MPa**
→ **APRR = 2.5 MPa/min, 65.3 MPa < Pdisp < 87.5 MPa**

The initial pressure is set to 20 bar = 2 MPa.

→ **P0 = 2 MPa.**

It can be noted that the refuelling time is estimated to **15 min.**

### 3.5 Head loss estimations

At the HRS station, the dispenser pressure is measured just before the breakaway device. Depending on the hose and nozzle selected, the kv value between the pressure measured and the nozzle is assumed to be:

- **kv> 0.2 $m^3/h$**
  → basic equipment for a HD H70 refuelling.
- **kv<0.6 $m^3/h$**
  → good equipment for a HD H70 refuelling.

Inside the vehicle, the head loss variation is assumed to be negligeable compared to the head loss amplitude selected for the station.

### 3.6 Results

In Figure 12 it can be seen in that:

1. The head loss between the dispenser and the tank impacts the mass flow rate. At the beginning of a refuelling, the mass flow is typically having a peak. More head loss in the piping tends to delay the mass flow peak.
2. The head loss between the dispenser and the tank impacts the final gas temperature. Between the lower kv and the largest kv, a difference of 6.7 °C is estimated. Hence, the lower kv (0.2 $m^3/h$) leads to 81.5 °C and the largest kv (0.6 $m^3/h$) leads to 74.8 °C.

The difference is a consequence of two phenomena:

- the head loss increases the injected temperature in the tank due to the Joule-Thomson effect. More head loss implies a warmer injection temperature.
- an early mass flow peak is generating an early temperature rise in the tank during the refuelling. This tends to increase the heat exchanged between the gas in the tank and the tank walls. Consequently, when more heat is transferred from the gas to the tank walls, the gas temperature at the end of the refuelling is reduced.

In term of SOC, both refuellings are very close: SOC=100.6 % for kv=0.2 $m^3/h$ and SOC=102,1% for kv=0.6 $m^3/h$.

This project has received funding from the European Union's HORIZON EUROPE research and innovation programme under grant agreement No. 101096028. The content of this publication is the sole responsibility of the Consortium partners listed herein and does not necessarily represent the view of the European Commission or its services.

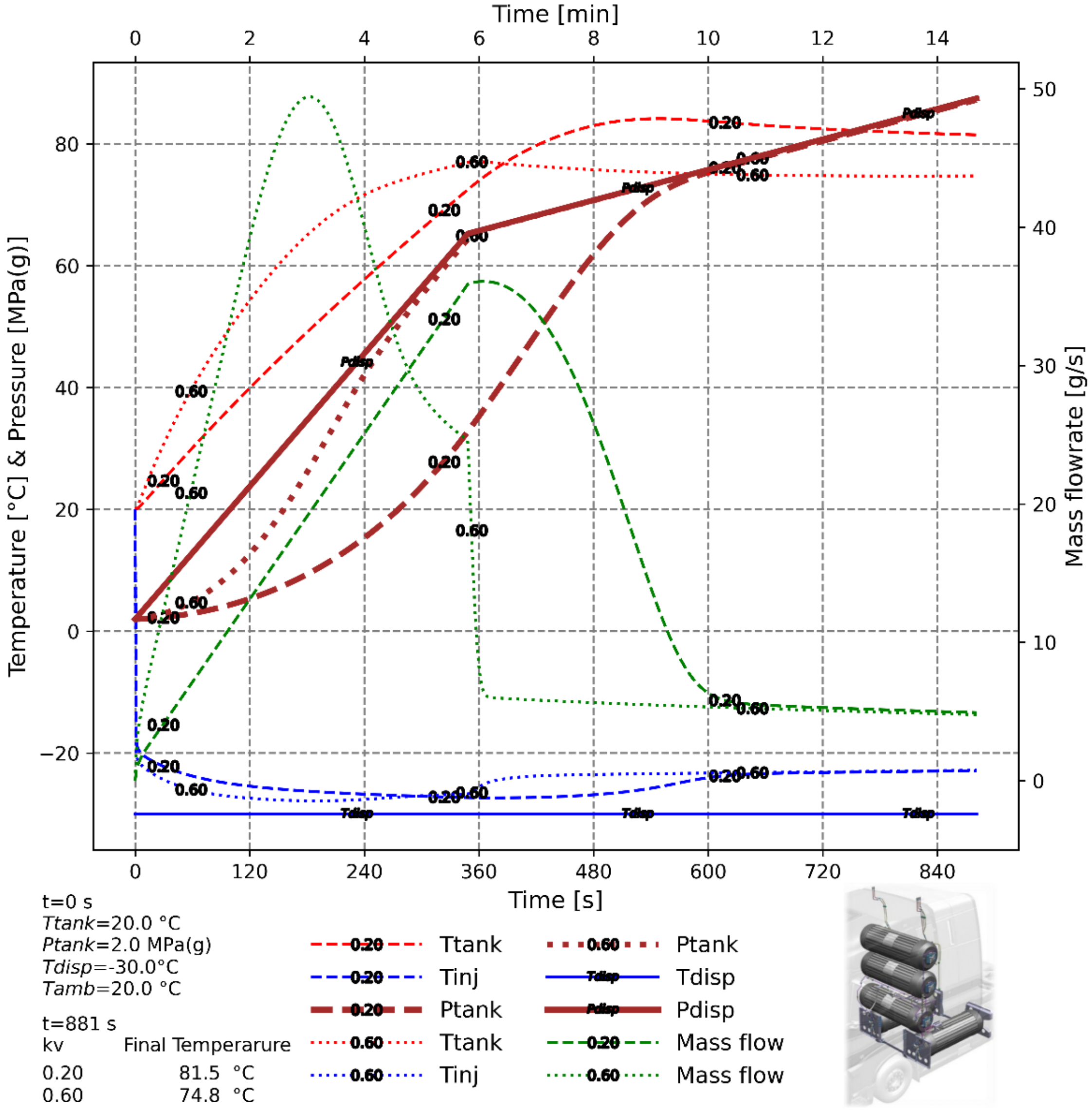


Figure 12: Simulation results of two refuelling cases using two different head loss coefficients kv between the dispenser and the tank: 0.2 m3/h and 0.6 m3/h.

# 4 Conclusion

It has successfully been identified and evaluated the most suitable hydrogen storage system for the FCEV demonstrator, aiming to achieve a 750 km range while minimising the impact on the vehicle's weight. The chosen solution, a compressed hydrogen storage system with five Type IV tanks operating at 700 bar has been selected based on market readiness, customer needs, and regulatory compliance.

A lot of simulations have been conducted to define and to optimise the power strategy between the fuel cell and battery, ensuring performance comparable to a baseline diesel truck. This activity is going on and will accompany the project during the complete development. Also, the refuelling process has been thoroughly investigated, with parametric and sensitivity analyses conducted using a dedicated simulation tool developed by ALSA.

As far as the simulation is concerning, the look-up table refuelling protocol from the standard SAE J2601-5 [17] uses enough temperature margin to prevent an overheating event despite the large range of existing kv. It appears safe to use this protocol during the first field-testing of the FCEV demonstrator. From this field testing, data will be collected.

A possible next step could be, from the pressure sensors located inside each tank, to extract the real head losses and to validate the modelling used in OneSOFIL.

Then, a parametric study could be performed to optimise the refuelling, to test advanced protocols or to investigate different refuelling scenarios (for instance a pre-cooler dysfunction).

The physical modelling used in OneSOFIL can also be employed during the defueling and stabilization phases of the tanks. This corresponds for the FCEV demonstrator to a driving phase or waiting phase respectively. For instance, the modelling can help calculating the hydrogen consumption during a driving phase or detecting a hydrogen leak during a waiting phase.

This project has received funding from the European Union's HORIZON EUROPE research and innovation programme under grant agreement No. 101096028. The content of this publication is the sole responsibility of the Consortium partners listed herein and does not necessarily represent the view of the European Commission or its services.

# 5 Bibliography


[1] Gómez J.A., Santos, D.M.F, «The Status of On-Board Hydrogen Storage in Fuel Cell Electric Vehicles,» 2023.

[2] «Fuels' parameters,» https://www.aidic.it/PositionPaperMobilit%C3%A0Idrogeno.pdf.

[3] «Hydrogen storage options and tanks,» https://www.awoe.net/Hydrogen-Storage-General.html.

[4] «Storage of liquid hydrogen,» https://sag.at/en/development/hydrogen/.

[5] E. Pizzutilo, T. Acher, B. Reuter, C. Will, «Subcooled Liquid Hydrogen Technology for Heavy Duty Trucks,» 2023.

[6] «Types of tank for H2 storage,» https://hyfindr.com/en/hydrogen-knowledge/hydrogen-tank.

[7] «Tanks type comparison,» https://stargatehydrogen.com/blog/hydrogen-storage-solutions/.

[8] «Hydrogen storage control unit description,» https://www.schaeffler-engineering.com/site.engineering/en/products/series_production/hydrogen_storage_control_unit_en/.

[9] «Hydrogen storage control unit,» https://www.bosch-mobility.com/en/solutions/control-units/hydrogen-storage-control-unit/.

[10] «Schematic of compressed H2 tank,» https://ecs-composite.com/hydrogen/?lang=en.

[11] SAE International Technical Standard, *Fueling Protocols for Light Duty Gaseous Hydrogen Surface Vehicles*, Issued March 2010, Revised May 2020, https://doi.org/10.4271/J2601_202005.

[12] T. Bourgeois, F. Ammouri, M. Weber, C. Knapik, «Evaluating the temperature inside a tank during a filling with highly-pressurized gas,» *International Journal of Hydrogen Energy*, vol. 40, n. 35, https://doi.org/10.1016/j.ijhydene.2015.01.096, pp. 11748-11755, 2015.

[13] T. Bourgeois, T. Brachmann, F. Barth, F. Ammouri, D. Baraldi, D. Melideo, B. Acosta-Iborra, D. Zaepffel, D. Saury, D. Lemonnier, «Optimization of hydrogen vehicle refuelling requirements,» *International Journal of Hydrogen Energy*, vol. 42, n. 19, https://doi.org/10.1016/j.ijhydene.2017.01.165, pp. 13789-13809, 2017.

[14] «HYTRANSFER - Pre-normative research for thermodynamic optimization of fast hydrogen transfer,» 2018, https://data.europa.eu/doi/10.2843/329142.

[15] «PRHYDE - Protocol for heavy duty hydrogen refuelling,» 2022, https://cordis.europa.eu/project/id/874997.

[16] «Properties of Nylon PA6,» https://designerdata.nl/materials/plastics/thermo-plastics/polyamide-6.

[17] SAE International Information Report, *High-Flow Prescriptive Fueling Protocols for Gaseous Hydrogen Powered Medium and Heavy-Duty Vehicles*, SAE Standard J2601/5_202402, 2024, https://doi.org/10.4271/J2601/5_202402.


This project has received funding from the European Union's HORIZON EUROPE research and innovation programme under grant agreement No. 101096028. The content of this publication is the sole responsibility of the Consortium partners listed herein and does not necessarily represent the view of the European Commission or its services.

## 6 Acknowledgment

**European Union's HORIZON EUROPE research and innovation programme**

This project has received funding from the European Union's HORIZON EUROPE research and innovation programme under grant agreement No. 101096028. The content of this publication is the sole responsibility of the Consortium partners listed herein and does not necessarily represent the view of the European Commission or its services.

**Project Partners:**

The author(s) would like to thank the partners in the project for their valuable comments on previous drafts and for performing the review.

| Participant No* | Participant short name | Participant organisation name | Country |
|---|---|---|---|
| 1 Coordinator | **AIT** | AIT Austrian Institute of Technology GmbH | AT |
| 2 | **IVECO** | IVECO SPA | IT |
| 3 | **FPT** | FPT Industrial SPA | IT |
| 4 | **IFPEN** | IFP Énergies nouvelles | FR |
| 5 | **POLITO** | Politecnico di Torino | IT |
| 6 | **LT** | Lead Tech SRL | IT |
| 7 | **VIL** | Villinger GmbH | AT |
| 8 | **CID** | Fundación CIDETEC | ES |
| 9 | **CTE** | CT Engineering GmbH | AT |
| 10 | **GLO** | GRUBER Logistics S.p.A. | IT |
| 11 | **BRE** | BREMBO SPA | IT |
| 12 | **IIT** | Istituto per Innovazioni Tecnologiche Bolzano S.c.a.r.l. | IT |
| 13 | **ALFI** | Air Liquide | FR |
| 14 | **FMF** | FPT Motorenforschung AG | CH |